Medical & Biological Engineering & Computing (2019) 57:123–134
https://doi.org/10.1007/s11517-018-1869-1

ORIGINAL ARTICLE

Cardiovascular assessment of supportive doctor-patient communication using multi-scale and multi-lag analysis of heartbeat dynamics

M. Nardelli[1] · A. Greco[1] · O. P. Danzi[2] · C. Perlini[2] · F. Tedeschi[2] · E. P. Scilingo[1] · L. Del Piccolo[2] · G. Valenza[1]

Received: 20 December 2017 / Accepted: 2 July 2018 / Published online: 14 July 2018
© International Federation for Medical and Biological Engineering 2018

Abstract
Emphatic doctor-patient communication has been associated with improved psycho-physiological well-being involving cardiovascular and neuroendocrine responses. Nevertheless, a comprehensive assessment of heartbeat linear and nonlinear dynamics throughout the communication of a life-threatening disease has not been performed yet. To this extent, we studied linear heartbeat dynamics through the extraction of time-frequency domain measurements, as well as heartbeat nonlinear and complex dynamics through novel approaches to compute multi-scale and multi-lag series analyses: namely, the multi-scale distribution entropy and lagged Poincaré plot symbolic analysis. Heart rate variability series were recorded from 54 healthy female subjects who were blind to the aim of the experiment. Participants were randomly assigned into two groups: 27 subjects watched a video where an oncologist discloses the diagnosis of a cancer metastasis to a patient, whereas the remaining 27 watched the same video including four additional supportive comments by the clinician. Considering differences between the beginning and the end of each communication video, results from non-parametric Wilcoxon tests demonstrated that, at a group level, significant differences occurred in heartbeat linear and nonlinear dynamics, with lower complexity during nonsupportive communication. Furthermore, a support vector machine algorithm, validated using a leave-one-subject-out procedure, was able to discern the supportive experience at a single-subject level with an accuracy of 83.33% when nonlinear features were considered, dropping to 51.85% when using standard HRV features only. In conclusion, heartbeat nonlinear and complex dynamics can be a viable tool for the psycho-physiological evaluation of supportive doctor-patient communication.

Keywords Supportive communication · Multi-scale entropy · Distribution entropy · Lagged Poincaré plot · Pattern recognition · Support vector machine

1 Introduction

Anxiety, apprehension, and feelings of nervousness are typical emotional responses associated with the communication of a negative clinical diagnosis [2], including stress and negative thoughts during its recall [2–5].

Previous studies highlighted how social support given by the clinician, including empathic communication, significantly reduces the secretion of stress hormones [6, 7], while improving patient's cardiovascular and neuroendocrine (i.e., immune-mediated inflammatory processes) profile [8, 9]. Particularly, a reduced physiological arousal as estimated through sympatho-vagal balance from heart rate variability (HRV) was associated with supportive communication after exposure to stress [10] rather than nonsupportive communication. Also, a significantly reduced skin conductance level during affective communication of the diagnosis of incurable cancer was found with respect to the standard condition [11]. Importantly, doctors also experience high stress during the pre-news delivery phase of breaking bad news interactions, as demonstrated by heart rate and electrodermal activity analyses [12]. Previous studies demonstrated

✉ M. Nardelli
mimma.nardelli@for.unipi.it

[1] Bioengineering and Robotics Research Centre E. Piaggio, Department of Information Engineering, School of Engineering, University of Pisa, Pisa, Italy

[2] Department of Neurological, Biomedical and Movement Sciences, University of Verona, Verona, Italy

www.manaraa.com

the link between electrodermal activity and stress, which was elicited using well-known tests including Mannheim Multicomponent Stress Test [13], and Stroop color word test [14].

Despite the aforementioned evidences, to our knowledge, no previous study has proposed a thorough assessment of heartbeat linear and nonlinear/complex dynamics in supportive vs. neutral doctor-patient communication. A proper psycho-physiological assessment of cardiovascular dynamics, in fact, should also account for measures with no intrinsic assumption of linearity (i.e., output of cardiac activity proportional to input stressors) and time-invariant properties [15], as suggested by recent reviews and guidelines [15–20]. Indeed, autonomic nervous system (ANS) control on cardiovascular activity has been widely recognized as nonlinear [21]. The effect on heart rate of a given vagal stimulation strongly depends on the "background level" of sympathetic stimulation occurring at the same time [21]; therefore, a vagal increase does not always result in a decrease of heart rate.

In this study, we took inspiration from the experimental protocol proposed by Sep et al. [11] to investigate ANS response throughout time-frequency and nonlinear/complex analyses of HRV series. Two groups of 27 women each were emotionally elicited through two different videos (ordinary vs. supportive) on a doctor-patient communication of an incurable breast cancer diagnosis, while continuously recording subject's electrocardiogram (ECG).

To comprehensively assess the effect of emphatic doctor-patient on heartbeat dynamics, we employed a multi-scale version of Distribution Entropy (DistEn) [20], i.e., Multi-scale DistEn (MDE), as well as a modified version of symbolic analysis originally proposed by Porta et al. [41] that is applied to lagged Poincaré plots (LPP), i.e., LPP_{symb} [22]. Among the plethora of HRV measures quantifying nonlinear and complex cardiac dynamics, in fact, DistEn has been recently proposed as a complexity index with a lower sensitivity to its free parameters than standard sample entropy, and has been proven effective with ultra-short time HRV series [20, 26]. Previous studies showed that several psycho-physiological states different from resting state are often associated with distinctive alterations in HRV multi-scaling properties, usually with an irregularity decrease especially at high scales [19, 23, 24]. To this extent, controversial findings were reported for heartbeat complexity modulation by aging [23–25]. Traditional entropy-based algorithms, as sample entropy and approximate entropy, quantify the regularity of a time series by evaluating the appearance of repetitive patterns [51]. The multi-scale entropy (MSE) method is based on the rationale that complex systems generally reveal long-range correlation structures over multiple temporal scales [61–63]. Therefore, MSE has been used to compare the degree of complexity between different time series [51]. On the other hand, DistEn implements the concept of "spacial structure" and can be considered as a measure of complexity also at the first scale [20, 26]. The MDE method proposed here applies the standard coarse-graining approach to the DistEn algorithm [19]. We adopted this procedure to study how the spatial complexity structure of a time series changes over different time scales, therefore investigating whether higher MDE scales may add further information about the complex dynamics of the cardiovascular system.

Furthermore, the reliability of LPP and LPP_{symb} approaches was demonstrated in RR interval series with a duration of 1 min or even less [22, 31, 54]. Note that LPPs were successfully employed to investigate changes in short- and long-term variability of HRV during pathological conditions, such as diabetes [27] and congestive heart failure [28], as well as physiological responses to meditation [29] and emotions [22, 30, 31].

To move beyond the group-level statistical analyses, in this study, we also exploited the aforementioned HRV metrics to automatically characterize the cardiac dynamics associated with ordinary vs. supportive communication at a single-subject level using nonlinear support vector machine (SVM) algorithm, validated through the leave-one-subject-out (LOSO) procedure. Methodological and experimental details, as well as results, discussion, and conclusions, follow.

2 Methods

2.1 Subjects recruitment, experimental protocol, and acquisition setup

To experimentally analyze the impact of different styles of communication, 60 healthy subjects were recruited at the University of Verona, Italy. After a preliminary visual inspection check, six signals, three from each group of subjects, were excluded because of artifacts in the ECG recording; thus, reported data regard 54 participants. In order to avoid confounding gender effects, only women were enrolled in the study. Eligible participants were able to speak fluent Italian and did not have previous cancer history. Subjects were randomly assigned to one of two groups of 27 participants: ordinary group (hereinafter, group O, aged 25 ± 8.8) and supportive group (hereinafter, group S, aged 26.1 ± 9.6). Each group was asked to watch one out of the two versions of a scripted video-vignette of a bad news consultation, in which physician's communication differed only for the presence of supportive comments. The randomization sequence followed for the allocation of the subjects into the two groups was generated using Stata 11.0 software. All participants were blind to the aim of the study and the condition they were assigned to. Participants' recruitment was

www.manaraa.com

carefully performed and the two groups of participants were comparable either in terms of socio-demographic characteristics or clinical, personality, and communication preferences. To verify the homogeneity of the groups in terms of emotional regulation, the Interpersonal Reactivity Index (IRI), which is a 28-item questionnaire measuring empathy [32], was administered to each subject. This scale provides four sub-scores; each of these sub-scales taps a separate aspect of the global concept of empathy:

- IRI-Fantasy: the tendency of the respondent to shift him/herself into feelings of fictional characters taken from books, movies, or plays;
- IRI-Perspective-taking: the ability of the respondent to adopt the perspective, or point of view, of other people;
- IRI- Empathic Concern: the tendency for the respondent to experience feelings of warmth, compassion, and concern for others undergoing negative experiences;
- IRI-Personal Distress: the capability to experience feelings of discomfort and anxiety when witnessing the negative experiences of others.

Since personality factors and mood states may affect emotional processing and regulation, subjects' anxiety level was quantified using the Spielberger State-Trait Anxiety Inventory (STAI) [60]. This scale is generally aimed at determining whether subjects present anxiety as a stable and persistent emotional state (trait anxiety), or as a temporary condition elicited by exogenous stimuli (state anxiety). Both STAI-trait and STAI-state questionnaires were administered before the experiment, whereas the STAI-state test only was administered after the video.

Both groups were asked to watch a video. Throughout this video, a middle-aged male physician disclosed the diagnosis of a breast cancer metastasis to a 42-year-old woman, who was accompanied by her husband. Diagnosis, prognosis, technical details, consequences of the palliative treatment, and life expectancy were discussed during the physician-patient consultation. The dialog was preceded by a scene in which the patient introduces herself and expresses her feelings towards the upcoming consultation (priming scene), to facilitate the identification of the participants with the video-patient. The contents of both O and S videos were identical concerning the provided information, with the only difference of four additional supportive comments which started to be expressed at 5:35, after the beginning of the S video. Such comments were as follows:

- "But whatever action we do take, and however that develops, we will continue to take good care of you. We will be with you all the way."
- "We will do and will continue to do our very best for you."
- "And whatever happens, we will never let you down. You are not facing this on your own."
- "I completely understand your reluctance. We'll look at this decision together carefully and we'll pay attention to your concerns."

In addition, both videos were anticipated and followed by 4 min of aquarium images, which were used as neutral visual elicitation sessions to promote the relaxation of the subjects. This allowed to gather stable physiological recordings at resting state. The ordinary-communication video lasted 9 min and 41 s; the duration of the supportive-communication video was 10 min and 19 s. No so-called filler communication was used to compensate for the difference in length between videos as it could not be ordinary and subject's reaction to the video could unintentionally be influenced.

Throughout the experimental protocol, ECG signals were recorded by means of ECG100C Electrocardiogram Amplifier from BIOPAC Inc., with a sampling rate of 500 Hz. To obtain the RR series from the ECG, we used the automatic algorithm developed by Pan-Tompkins [33]. Artifacts and ectopic beats were corrected through the use of Kubios HRV software [34]. In Fig. 1, an overview of the experimental protocol is shown.

2.2 Methodology of signal processing

HRV processing was applied considering the following time windows:

- Vid1, including the first 110 s of the doctor-patient communication, after the 4 min of aquarium;
- Vid2, including the last 110 s of the doctor-patient communication, before the last 4 min of aquarium. For the group S, this window corresponds to the session

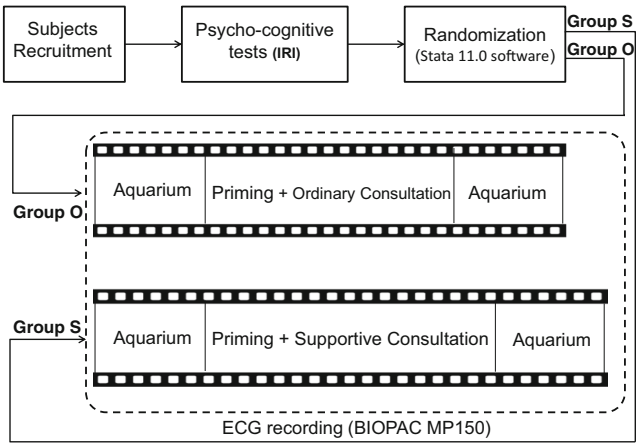

Fig. 1 Overall scheme of the experimental protocol. O, ordinary communication; S, supportive communication

www.manaraa.com

immediately after the supportive comments provided by the doctor.

From each RR series, we extracted features quantifying cardiac linear and nonlinear dynamics. Concerning the latter, two methods were used: multi-scale distribution entropy (MDE) and lagged Poincaré plots and symbolic analysis LPP_{symb}.

2.2.1 HRV standard features

Standard HRV measures are defined in the time and frequency domains.

Two features were computed in the time-domain: the mean value (RR mean) and standard deviation (RR std) of the RR intervals [35].

Features defined in the frequency domain were calculated using the Smoothed Pseudo Wigner-Ville Distribution [36]. On the time-frequency representation, using a nonoverlapping 5-s sliding window, we took into account the median power spectral density within low frequency bandwidth (LF power), ranging between 0.04 and 0.15 Hz, and the median power spectral density within high-frequency bandwidth (HF power), comprising frequencies between 0.15 to 0.4 Hz [53]. Then, we computed the frequency with maximum amplitude (LF peak and HF peak), the powers of LF and HF bands in normalized units, i.e., LF power n.u. ($\frac{\text{LF power}}{\text{LF power} + \text{HF power}}$) and HF power n.u. ($\frac{\text{HF power}}{\text{LF power} + \text{HF power}}$), and the ratio between LF power and HF power ($\frac{\text{LF power}}{\text{HF power}}$) [35]. In this study, we consider therefore a total of nine standard HRV features.

2.2.2 HRV multi-scale distribution entropy

A total of nine features were investigated by exploiting the theory of $DistEn$ [20, 37].

DistEn is a measure of complexity, and is calculated starting from the empirical probability distribution function.

Specifically, for a given time series of N samples $\{u(i), 1 \leq i \leq N\}$, *DistEn* algorithm is computed as follows:

- The phase-space of the system represented by the time series $u(i)$ is reconstructed through the embedding dimension m, $(N - m)$ vectors X_i^m built from the original series as follows:

$$X_i^m = u(i), u(i+1), \ldots, u(i+m-1), 1 \leq i \leq N-m.$$

- Considering each vector Xi^m, the distances between this vector and every vector X_j^m are computed using the formula of the Chebyshev distance:

$$d_{ij}^m = \max |X_i^m - X_j^m| : 1 \leq j \leq (N-m), j \neq i \quad (1)$$

The distance matrix D is constructed using the distances d_{ij}. The total amount of elements in the distance matrix D except its main diagonal is therefore $(N - m) \times (N - m - 1)$ [20].

- The histogram approach is used to estimate the empirical probability distribution function. The elements of D are divided into B bins and the corresponding histogram is obtained. At each bin t ($t = 1, \ldots, B$) of the histogram, its probability p_t is computed as

$$p_t = \frac{\text{count in bin t}}{\text{total number of elements in matrix D}} \quad (2)$$

To reduce bias, elements with $i = j$ were excluded from the estimation of the empirical probability distribution function.

- The *DistEn* of $u(i)$ is computed by normalizing the classical Shannon Entropy:

$$DistEn(m, B) = -\frac{1}{\log_2(B)} \sum_{t=1}^{B} p_t \log_2(p_t) \quad (3)$$

where m is the embedding dimension, B is the number of bins used to construct the histogram, and p_t is the probability of each bin in the histogram.

In this study, we applied the *DistEn* algorithm in a multi-scale fashion; therefore, using a coarse-graining process. Coarse-grained time series were constructed from the original RR series by averaging the data points within nonoverlapping windows of increasing length, τ.

Given the time series $\{u_1, \ldots, u_i, \ldots, u_N\}$ and a scale factor τ, each element of a coarse-grained series $\{y^{(\tau)}\}$ is calculated using the equation:

$$y_j^{(\tau)} = \frac{1}{\tau} \sum_{i=(j-1)\tau+1}^{j\tau} u_i, 1 \leq j \leq N/\tau \quad (4)$$

The length of each coarse-grained time series is equal to the length of the original time series divided by τ.

DistEn algorithm was demonstrated to be a reliable measure of complexity for ultra-short series [20, 26]. However, given the duration of the RR interval series considered in our experimental protocol (110 s), we explored only the first three scales, i.e., using a range of τ between 1 and 3. For each τ, we calculated the value of *DistEn* of the corresponding scaled series. Also, the mean of *Disten* values in the three scales (MDE_{mean}) was considered as descriptor of changes in heartbeat dynamics.

2.2.3 HRV lagged Poincaré plots and symbolic analysis (LPP_{symb})

A scatterplot of the lagged RR interval series, RR_{n+M}, against the series RR_n, was built along different lags M,

www.manaraa.com

using the range $1 \leq M \leq 30$. According to the ellipse-fitting technique, for each M value, an imaginary ellipse is fitted on the scatterplot and used to extract some geometrical parameters [22, 31, 38]:

- SD1: the standard deviation of the points calculated along the direction perpendicular to the line-of-identity $RR_{n+M} = RR_n$;
- SD2: the standard deviation of the points along the line-of-identity $RR_{n+M} = RR_n$;
- SD12 ($SD12 = SD1/SD2$): the ratio between SD1 and SD2;
- S ($S = \pi \times SD1 \times SD2$): the area of an imaginary ellipse with axes SD1 and SD2 [39, 40].

To minimize the loss of information by accounting for the phase space points which are outside the ellipse, we here propose two novel LPP quantifiers: namely, the mean (M_d) and the standard deviation (S_d) of the distances between all the points of each phase space point and its centroid. At each lag, the centroid Cd was defined as follows:

$$\begin{cases} Cd_x = \frac{1}{N-M}\sum_{n=1}^{N-M} RR_n \\ Cd_y = \frac{1}{N-M}\sum_{n=M+1}^{N} RR_n \end{cases} \quad (5)$$

where N is the total number of RR intervals in the series.

Once the geometrical distances d_{P_n} between all the phase space points P_n of the Poincaré plot and the centroid were calculated, we computed the mean and the standard deviation of the distribution of these distances:

$$M_d = \frac{1}{N-M}\sum_{n=1}^{N-M} d_{P_n}$$
$$S_d = \sqrt{\frac{\sum_{n=1}^{N-M}(d_{P_n} - M_d)^2}{N-M-1}} \quad (6)$$

In Fig. 2, the LPP quantifiers are shown: on the left, we report an example on the ellipse-fitting approach, with the two axes (SD1 and SD2); whereas on the right one, distance d_{P_n} between a LPP point and the centroid is traced. Finally, to quantify changes in LPP trends throughout different lags

Table 1 Summary of the HRV features used in this study

HRV features		
Standard analysis	Time domain	RR mean
		RR std
	Frequency domain	LF peak
		HF peak
		LF power
		HF power
		LF nu
		HF nu
		LF/HF
Nonlinear analysis	MDE	MDE_1
		MDE_2
		MDE_3
		MDE_{mean}
	LPP_{symb}	$SD1_{LPPsymb}$
		$SD2_{LPPsymb}$
		$SD12_{LPPsymb}$
		$S_{LPPsymb}$
		$Md_{LPPsymb}$
		$Sd_{LPPsymb}$

M, we applied a modified version of the original symbolic analysis method proposed by Porta et al. [41].

After extracting the LPP quantifiers over the first 30 lags, we divided the amplitude range of each M_d and S_d (as well as the other LPP parameters) in $\psi = 12$ equal levels, with a resolution of $(RR_{max}\text{-}RR_{min})/\psi$. We then assigned a symbol from 0 to 11, from the lowest to the highest, to each level.

The technique of the delayed coordinates was used to transform the RR^{ψ} series into a sequence of patterns of L = 3 symbols: $RR_{\psi,L} = \{RR_{\psi,L}(i), i = L, \ldots, N\}$ with $RR_{\psi,L}(i)$ [$RR_{\psi}(i)$, $RR_{\psi}(i - 1)$, …, $RR_{\psi}(i - L + 1)$]. Then, the variability in the amplitude of LPP quantifiers over the lags was categorized by counting the total number of three-symbol patterns with at least one variation in the symbol values. We evaluated the rate of occurrence of these patterns by computing their percentage in relation to the

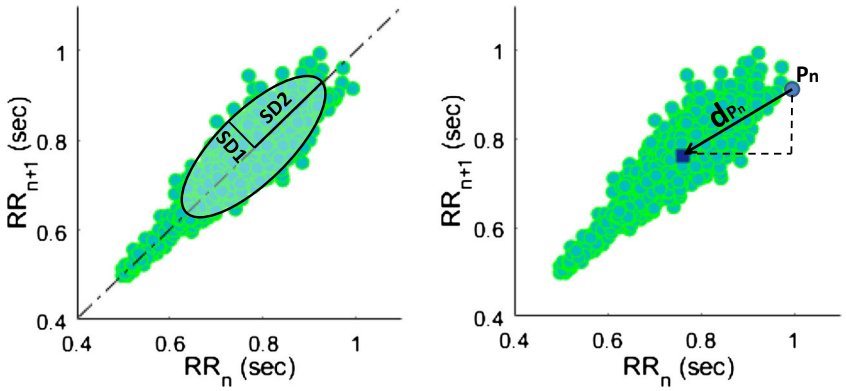

Fig. 2 An example of LPP quantifiers for the first lag ($M = 1$). In the left panel, the ellipse-fitting approach is shown with the two axes (SD1 and SD2); whereas on the right panel, the distance d_{P_n} between a LPP point and the centroid is traced

www.manaraa.com

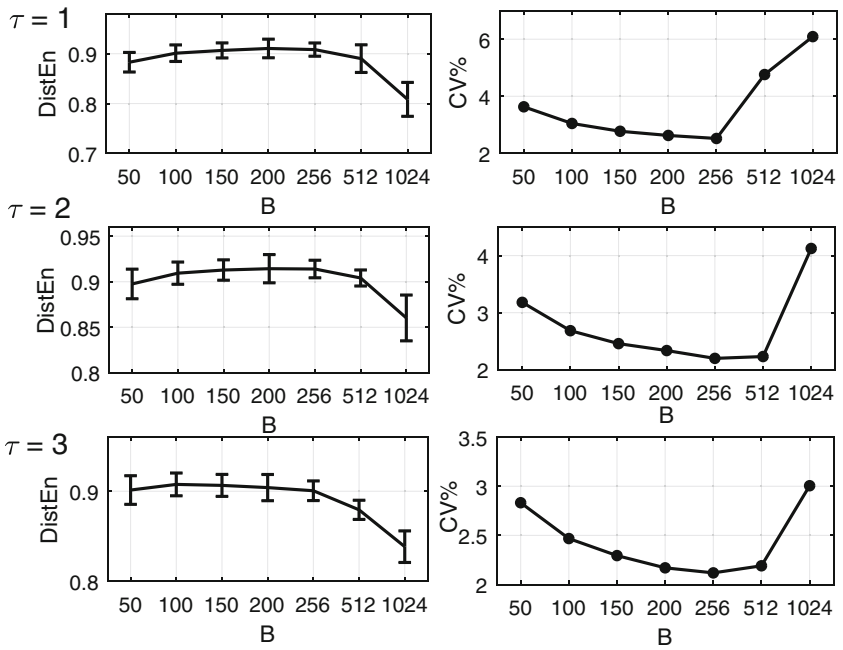

Fig. 3 Graphical representation of $DistEn$ values as a function of B. Median and MAD values of $DistEn$ are shown in the left column, whereas CV% is reported on the right column

total number of patterns. Therefore, as features, a total of six relative rates of the occurrence of three symbol patterns with at least one variation were extracted from a given RR interval series, one for each LPP quantifier: $SD1$, $SD2$, S, and $SD12$, as well as M_d and S_d.

Table 1 lists the HRV features used in this study.

2.2.4 Statistical analysis

We computed two kinds of statistical analyses: an inter-group comparison to investigate differences between the two groups (O vs. S) on IRI and STAI psychological scores, and an intra-group comparison between Vid1 and Vid2 sessions within each group on HRV metrics. Mann-Whitney nonparametric test was used to assess inter-group differences, whereas Wilcoxon nonparametric tests to assess intra-group ones. All p values obtained through multiple comparisons have been corrected using an adaptive linear step-up procedure to control false discovery rate [47]. Note that the session Vid2 corresponds to the time right after the empathic comments in the video watched by the S group.

2.2.5 Pattern recognition

Pattern recognition analysis aimed to automatically discern the cardiovascular dynamics associated with emphatic vs. standard doctor-patient communication at a single-subject level. Each HRV feature calculated within session Vid2 was normalized by subtracting the corresponding value calculated within Vid1, and taken as an input of the classification algorithm.

We chose a C-SVM [42] with a sigmoid function kernel, validated through a LOSO procedure. A feature selection procedure, including a correlation bias reduction strategy within the training set of $N-1$ subjects, where N is the total

Table 2 Summary of MDE and LPP_{symb} parameters used to generate complexity markers

	Symbol	Description	Value
MDE parameters	m	Embedding dimension	2
	B	Equally spaced bins in which the distance matrix D is divided	256
	τ	Scale factor	$1 \leq \tau \leq 3$
LPP_{symb} parameters	M	Number of lags	$1 \leq M \leq 30$
	ψ	Equally spaced levels in which the amplitude range is divided	12
	L	Number of symbols for each patterns	3

Table 3 Statistical results from Mann-Whitney tests on IRI scores

	Group O (median ± MAD)	Group S (median ± MAD)	p value
IRI-fantasy	26 ± 4	25 ± 2	0.18
IRI-Empathic concern	28 ± 3	29 ± 2	0.43
IRI-Perspective-taking	23 ± 3	26 ± 3	0.08
IRI-Personal distress	18 ± 3	19 ± 3	0.22

www.manaraa.com

Table 4 Statistical results from Mann-Whitney statistical tests on STAI scores related to the questionnaires filled before and after the experiment

		Group O (median ± MAD)	Group S (median ± MAD)	p value
PRE	STAI-State	37 ± 4	36 ± 3	0.74
	STAI-Trait	43 ±5	46 ±5	0.17
POST	STAI-State	39 ± 7	40 ± 5	0.27

number of participants, was carried out [43]. All of the algorithms were implemented by using MATLAB v8.6 endowed with an additional toolbox for statistical mapping, i.e., LIBSVM [44].

3 Experimental results

As *DistEn* remains stable in physiological signals over $m = [2 - 5]$, changing as a function of the number of samples and B [26], we firstly report on how *DistEn* calculated in our 108 RR interval series of 110 s changes as a function of B. Left column plots in Fig. 3 show *DistEn* trend (median and median absolute deviation) for the three value of scale factor τ, with $B = [50, 100, 150, 200, 256, 512, 1024]$, whereas the percentage value of the coefficient of variation, calculated as $CV\% = \frac{\sigma}{\mu} \times 100$ (where σ and μ are the standard deviation and the mean of all $DistEn$ values, respectively) are shown in the right column. These results suggest that the median values of $DistEn$ were almost stable in the range $B = [100, 256]$, while they tended to decrease at $B = 512$ and, more significantly, at $B = 1024$. Minimum values of the coefficient of variation were at $B = 256$. For these reasons, the parameters for the computation of $DistEn$ for further analyses were fixed for the three scales at the values of $B = 256$ and $m = 2$, as shown in Table 2.

Tables 3 and 4 show the p values obtained from Mann-Whitney statistical tests, together with the median and median absolute deviation (MAD) for each group, on the four IRI sub-scales and the two STAI sub-scales. No statistical differences were found between the ordinary and supportive groups.

Table 5 shows results from the statistical analysis on heartbeat linear and nonlinear dynamics. Wilcoxon statistical test was applied for each group between HRV estimates from Vid1 and Vid2. Both groups presented statistical differences between Vid1 and Vid2 for the frequency parameters. Nevertheless, the increase of LF/HF and the

Table 5 HRV metrics calculated during Vid1 and Vid2 sessions for O and S groups, expressed as (median ± MAD)

	Group O		Group S	
	Vid1 (med. ± MAD)	Vid2 (med. ± MAD)	Vid1 (med. ± MAD)	Vid2 (med. ± MAD)
RR mean	0.76 ± 0.07	0.78 ± 0.04	*0.82 ± 0.08*	*0.79 ± 0.07*
RR std	0.05 ± 0.01	0.05 ± 0.01	0.04 ± 0.01	0.04 ± 0.01
LF peak	0.07 ± 0.03	0.08 ± 0.02	0.06 ± 0.02	0.07 ± 0.03
HF peak	0.23 ± 0.05	0.23 ± 0.07	0.28 ± 0.03	0.27 ± 0.04
LF power	0.09 ± 0.06	0.09 ± 0.06	0.05 ± 0.05	0.04 ± 0.03
HF power	0.03 ± 0.02	0.02 ± 0.01	*0.03 ± 0.03*	*0.02 ± 0.02*
LF nu	*0.61 ± 0.20*	*0.81 ± 0.11*	*0.62 ± 0.20*	*0.72 ± 0.12*
HF nu	*0.39 ± 0.20*	*0.19 ± 0.11*	*0.38 ± 0.20*	*0.28 ± 0.12*
LF/HF	*1.55 ± 1.22*	*4.32 ± 3.23*	*1.61 ± 1.17*	*2.56 ± 2.10*
MDE_1	*0.92 ± 0.01*	*0.91 ± 0.01*	0.90 ± 0.02	0.91 ± 0.01
MDE_2	0.92 ± 0.01	0.92 ± 0.01	0.90 ± 0.02	0.91 ± 0.01
MDE_3	0.90 ± 0.01	0.90 ± 0.01	0.90 ± 0.02	0.91 ± 0.01
MDE_{mean}	0.91 ± 0.003	0.91 ± 0.01	0.90 ± 0.01	0.91± 0.02
$SD1_{LPPsymb}$	53.57 ± 3.57	50.00 ± 3.57	60.71 ± 3.57	57.14 ± 10.71
$SD2_{LPPsymb}$	50.00 ± 7.14	53.57 ± 7.14	57.14 ± 7.14	57.14 ± 10.71
$SD12_{LPPsymb}$	50.00 ± 7.14	53.57 ± 7.14	60.71 ± 7.14	57.14 ± 7.14
$S_{LPPsymb}$	57.14 ± 14.29	50.00 ± 14.29	64.29 ± 10.71	64.29 ± 10.71
$Md_{LPPsymb}$	*57.14 ± 10.71*	*64.29 ± 3.57*	67.86 ± 7.14	60.71 ± 7.14
$Sd_{LPPsymb}$	60.71 ± 7.14	67.86± 3.57	71.43 ± 7.14	64.29 ± 3.57

Italicized metrics indicate significant p values ($p < 0.05$) from the Wilcoxon statistical test between the two sessions

www.manaraa.com

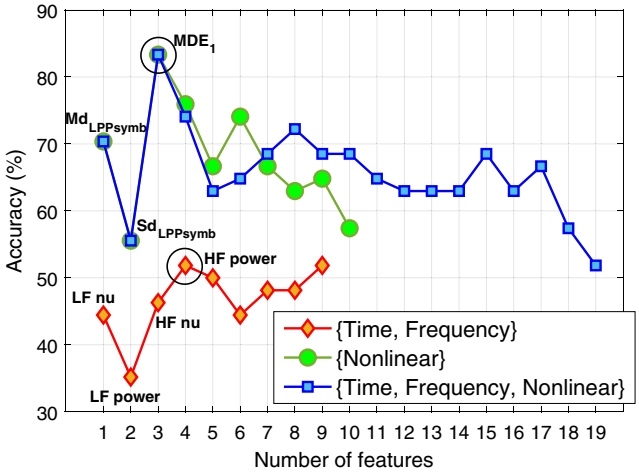

Fig. 4 Recognition accuracy for the S vs. O classification obtained through the LOSO SVM-RFE procedure, shown as a function of the feature number, for the three datasets. Black circles indicate the highest accuracies

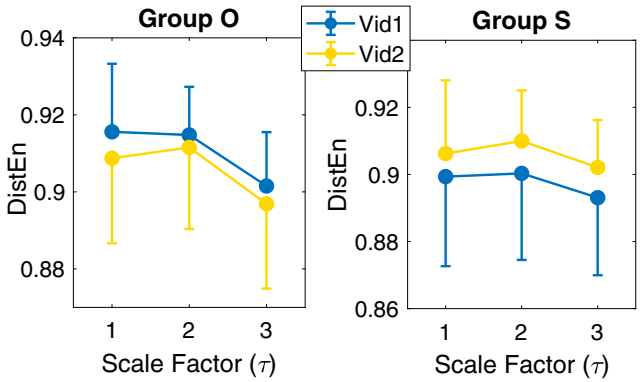

Fig. 5 *DistEn* as a function of the scale factor τ for groups S and O. The values obtained are reported as mean and std

decrease of HF power n.u. are more significant in group O than those in group S. Moreover, the values of $Md_{LPPsymb}$ resulted statistically different in group O.

The pattern recognition algorithm described in Section 2.2.5 was applied to automatically discern subjects experiencing either supportive or ordinary doctor-patient communication. The pattern recognition procedure was applied for three different feature sets:

- Dataset 1: Comprising time-frequency and nonlinear/complexity features;
- Dataset 2: Nonlinear/complexity features;
- Dataset 3: Comprising time-frequency features.

Figure 4 shows the recognition accuracy as a function of the number of features ranked using the LOSO SVM-RFE procedure, for the three input datasets.

Table 6 O vs. S confusion matrices using HRV features

		Group O	Group S
Group O	Time-frequency-nonlinear	*81.4815*	18.5185
	Time-frequency	51.8519	48.1481
	Nonlinear	*81.4815*	18.5185
Group S	Time-frequency-nonlinear	14.8148	*85.1852*
	Time-frequency	48.1481	51.8519
	Nonlinear	14.8148	*85.1852*

Italicized values indicate the highest classification accuracy for each feature group

Values in italics are the highest rates of classification successes, in terms of true positive and true negative, related in this case to the nonlinear dataset and to the total dataset

The lowest accuracy was obtained when time-frequency parameters only were taken into account. The classification accuracy was as low as 51.85% using the following four features: LF nu, LF power, HF nu, and HF power.

Considering features quantifying heartbeat nonlinear/complex dynamics exclusively, an accuracy of 83.33% was achieved using three features: $Md_{LPPsymb}$, $Sd_{LPPsymb}$, and MDE_1. When all of the features were taken as input, the LOSO SVM-RFE procedure provides a maximum accuracy of 83.33%, selecting the same three nonlinear features.

Table 6 shows the confusion matrices from the SVM classification of the O vs. S groups using the three datasets. They refer to the maximum accuracy obtained for each dataset.

MDE values for the two groups during Vid1 and Vid2 are reported in Fig. 5.

4 Discussion and conclusion

We studied linear and nonlinear heartbeat dynamics in two groups of healthy women watching a bad-news consultation video, where clinical information was provided with or without supportive comments by the clinician. The experimental procedure and video were already validated in the literature [11]. To our knowledge, our study is the first attempt to investigate a comprehensive set of HRV measures during a doctor-patient communication.

We hypothesized that the different heartbeat complexity quantifiers calculated over different time scales would provide meaningful information on the emotional reaction of the subject, because of the continuous brain-heart interplay. Accordingly, we calculated HRV features defined in the time and frequency domains, as well as from two nonlinear dynamics methods. This study is an extension of [52], in which we investigated heartbeat dynamics from

www.manaraa.com

34 subjects divided into the two groups, and demonstrated the effectiveness of the multi-lag analysis through the LPP_{symb}. Here, we increased the number of participants to 54, and applied the LPP_{symb} also to M_d and S_d quantifiers of LPP, together with a multi-scale analysis of the RR interval series. Specifically, we adopted a multi-scale approach for the quantification of the degree of complexity at different time scales, i.e., the multi-scale DistEn (MDE), because of its ability to quantify complexity in ultra-short series [20].

We chose to employ the LPP_{symb} method instead of computing the traditional symbolic indexes directly from RR interval series [49, 50, 58] because the LPP_{symb} approach investigates the symbolic dynamics in a hyperdimensional space given by the first M Poincaré return maps, where M is the range of lags. The application of this approach on both linear-related Poincaré plot quantifiers (SD1 and SD2 [59]) and all the other quantifiers described in Section 2.2 allowed us to investigate heartbeat dynamics comprehensively from the beat-to-beat structure displayed by the LPP over 30 lags. Note that, in a previous study, we demonstrated the reliability of LPP quantifiers extracted from RR interval series comprising 35–60 samples, along with its discriminant power in affective elicitation protocols [31]. Therefore, it is possible to consider 100 samples enough to derive reliable LPP parameters. Concerning the computation of DistEn, we explored its dependence on the value of parameter B, before applying it on the scaled series. We investigated seven values of B in the range [50, 1024] and we chose $B = 256$, which showed the lowest coefficient of variation for our RR series (see Fig. 3).

We recruited female participants only, therefore avoiding gender differences and biases in the assessment of ANS responses to supportive communication.

Non-parametric statistical analysis on IRI and STAI questionnaires demonstrated that the ordinary communication (O) and supportive (S) communication groups were not different in terms of feeling empathy and anxiety. Statistical analyses on heartbeat dynamics suggested a higher sympathetic activation, after the video elicitation, in subjects of the O group than S ones. This is suggested by the different magnitudes of increase/decrease of HRV frequency domain parameters in the groups, as well as by the reduction of heartbeat complexity observed in the O group (see Fig. 5). Note that recent evidences demonstrated how a sympathetic modulation on cardiovascular variability can be assessed through multi-scale entropy analysis [45, 46]. In previous studies, a progressive decrease of complexity was found in humans during an experimental protocol known to produce a gradual shift of the sympathovagal balance toward sympathetic activation, i.e., as a function of the tilt table inclination [55], and in rats during an increased sympathetic modulation, acting as a negative factor for the overall cardiovascular complexity regulation [56]. On the other hand, higher complexity was associated with good affective balance and healthier mental states [48].

To move from a group level to a single subject-level of analysis, a pattern recognition procedure based on SVM-RFE algorithm was applied to automatically discern heartbeat dynamics gathered from a subject experiencing a specific psycho-physiological state. Our results confirm the crucial role of heartbeat nonlinear and complex dynamics in characterizing supportive doctor-patient communication. Highest recognition accuracy between groups has been achieved, in fact, when MDE and LPP_{symb} measures were taken into account.

At a speculation level, our results link empathic doctor-patient communication to the so-called central autonomic network [1], through which the brain controls visceromotor, neuroendocrine, pain, and behavioral responses. It is reasonable, in fact, that the multi-feedback and cross-system loops generating heartbeat complex dynamics [21] are also influenced by the paraventricular and other hypothalamic nuclei containing mixed neuronal populations that control specific subsets of preganglionic sympathetic and parasympathetic neurons.

Our study presents some limitations, which may represent the starting point of future endeavours in the fields of HRV nonlinear analysis, and the assessment of autonomic dynamics during empathic communication. First, a detailed study on the reliability of DistEn also in time series shorter than 50 samples (lowest limit studied in the literature [20, 26]) should be performed. In this way, the effects of sympathetic activation on heartbeat complexity could be properly investigated. Also, the uniform binning procedure used in the MDE complexity estimation could affect the experimental results. Future research is needed to properly investigate these potential biases, eventually testing previously proposed correction procedures [57]. Further research is also needed to test possible biases related to the coarse graining procedure. Concerning the experimental protocol, a limitation is represented by the involvement of healthy subjects. Indeed, it would be very difficult to study ANS dynamics in subjects who are actually affected by cancer, and are monitored the very first time this bad news is received. Therefore, we state that our study dealt with highly arousing, highly unpleasant emotional elicitation whose associated ANS dynamics might be affected by the presence of emphatic communication. Finally, as we assessed female subjects exclusively, the assessment of psycho-physiological changes during emphatic communication in male subjects would be useful to investigate possible gender differences.

www.manaraa.com

References

1. Benarroch EE (1993) The central autonomic network: functional organization, dysfunction, and perspective. InMayo Clinic Proceedings 68(10):988–1001. Elsevier
2. Jansen J, van Weert JC, de Groot J, van Dulmen S, Heeren TJ, Bensing JM (2010) Emotional and informational patient cues: the impact of nurses' responses on recall. Patient Educ Couns 79(2):218–224
3. Kessels RP (2003) Patients' memory for medical information. J R Soc Med 96(5):219–222
4. van der Meulen N, Jansen J, van Dulmen S, Bensing J, van Weert J (2008) Interventions to improve recall of medical information in cancer patients: a systematic review of the literature. Psycho-Oncology 17(9):857–868
5. Gabrijel S et al (2008) Receiving the diagnosis of lung cancer: patient recall of information and satisfaction with physician communication. J Clin Oncol 26(2):297–302
6. Adler HM (2002) The sociophysiology of caring in the doctor-patient relationship. J Gen Intern Med 17(11):883–890
7. Fogarty LA, Curbow BA, Wingard JR, McDonnell K, Somerfield MR (1999) Can 40 seconds of compassion reduce patient anxiety? J Clin Oncol 17(1):371–371
8. Gerin W, Pieper C, Levy R, Pickering TG (1992) Social support in social interaction: a moderator of cardiovascular reactivity. Psychosom Med 54(3):324–336
9. Uchino BN (2006) Social support and health: a review of physiological processes potentially underlying links to disease outcomes. J Behav Med 29(4):377–387
10. Ono M, Fujita M, Yamada S (2009) Physiological and psychological responses to expressions of emotion and empathy in post-stress communication. J Physiol Anthropol 28(1):29–35
11. Sep MS et al (2014) The power of clinicians' affective communication: How reassurance about non-abandonment can reduce patients' physiological arousal and increase information recall in bad news consultations. an experimental study using analogue patients. Patient Educ Couns 95(1):45–52
12. Shaw J, Brown R, Dunn S (2015) The impact of delivery style on doctors' experience of stress during simulated bad news consultations. Patient Educ Couns 98(10):1255–1259
13. Reinhardt T, Schmahl C, Wüst S, Bohus M (2012) Salivary cortisol, heart rate, electrodermal activity and subjective stress responses to the mannheim multicomponent stress test (mmst). Psychiatry Res 198(1):106–111
14. Svetlak M, Bob P, Cernik M, Kukleta M (2010) Electrodermal complexity during the stroop colour word test. Autonomic Neuroscience: Basic and Clinical 152(1):101–107
15. Captur G, karperien AL, Hughes AD, Francis DP, Moon JC (2016) The fractal heartï¡œembracing mathematics in the cardiology clinic. Nat Rev Cardiol 14(1):nrcardio–2016
16. Voss A, Schulz S, Schroeder R, Baumert M, Caminal P (2009) Methods derived from nonlinear dynamics for analysing heart rate variability. Philosophical Transactions of the Royal Society of London A: Mathematical, Physical and Engineering Sciences 367(1887):277–296
17. Sassi R, Cerutti S, Lombardi F, Malik M, Huikuri HV, Peng C-K, Schmidt G, Yamamoto Y, Reviewers: D, Gorenek B et al (2015) Advances in heart rate variability signal analysis: joint position statement by the e-cardiology esc working group and the european heart rhythm association co-endorsed by the asia pacific heart rhythm society. EP Europace 17(9):1341–1353
18. Goldberger AL, Amaral LA, Hausdorff JM, Ivanov PC, Peng C-K, Stanley HE (2002) Fractal dynamics in physiology: alterations with disease and aging. Proc Natl Acad Sci 99(suppl 1):2466–2472
19. Costa M, Goldberger AL, Peng C-K (2002) Multiscale entropy analysis of complex physiologic time series. Phys Rev Lett 89(6):068102
20. Li P, Liu C, Li K, Zheng D, Liu C, Hou Y (2015) Assessing the complexity of short-term heartbeat interval series by distribution entropy. Med Biol Eng Comput 53(1):77–87
21. Sunagawa K, Kawada T, Nakahara T (1998) Dynamic nonlinear vago-sympathetic interaction in regulating heart rate. Heart Vessel 13(4):157–174
22. Nardelli M, Greco A, Valenza G, Lanata A, Bailón R, Scilingo E (2017) A novel heart rate variability analysis using lagged poincaré plot: A study on hedonic visual elicitation, In: Engineering in medicine and biology society (EMBC), 2017 39th Annual International Conference of the, IEEE. IEEE, pp 2300–2303
23. Goldberger AL, Peng C-K, Lipsitz LA (2002) What is physiologic complexity and how does it change with aging and disease? Neurobiol Aging 23(1):23–26
24. Wang J, Ning X, Ma Q, Bian C, Xu Y, Chen Y (2005) Multiscale multifractality analysis of a 12-lead electrocardiogram. Phys Rev E 71(6):062902
25. Schmitt DT, Ivanov PC (2007) Fractal scale-invariant and nonlinear properties of cardiac dynamics remain stable with advanced age: a new mechanistic picture of cardiac control in healthy elderly. Am J Physiol Regul Integr Comp Physiol 293(5): R1923–R1937
26. Karmakar C, Udhayakumar RK, Li P, Venkatesh S, Palaniswami M (2017) Stability, consistency and performance of distribution entropy in analysing short length heart rate variability (HRV) signal. Front Physiol 8:720
27. Contreras P, Canetti R, Migliaro ER (2006) Correlations between frequency-domain HRV indices and lagged poincaré plot width in healthy and diabetic subjects. Physiol Meas 28(1):85
28. Thakre TP, Smith ML (2006) Loss of lag-response curvilinearity of indices of heart rate variability in congestive heart failure. BMC Cardiovasc Disord 6(1):27
29. Goshvarpour A, Goshvarpour A, Rahati S (2011) Analysis of lagged poincaré plots in heart rate signals during meditation. Digital Signal Process 21(2):208–214
30. Nardelli M, Valenza G, Greco A, Lanata A, Scilingo EP (2015) Recognizing emotions induced by affective sounds through heart rate variability. IEEE Trans Affect Comput 6(4):385–394
31. Nardelli M, Greco A, Bolea J, Valenza G, Scilingo EP, Bailon R (2018) Reliability of lagged Poincaré plot parameters in ultra-short heart rate variability series: Application on affective sounds," IEEE Journal of Biomedical and Health Informatics
32. Davis MH (1980) A multidimensional approach to individual differences in empathy
33. Pan J, Tompkins WJ (1985) A real-time qrs detection algorithm. IEEE Trans Biomed Eng 3:230–236
34. Tarvainen MP, Niskanen J-P, Lipponen JA, Ranta-Aho PO, Karjalainen PA (2014) Kubios HRV–heart rate variability analysis software. Comput Methods Prog Biomed 113(1):210–220
35. Acharya UR, Joseph KP, Kannathal N, Lim CM, Suri JS (2006) Heart rate variability: a review. Med Biol Eng Comput 44(12): 1031–1051
36. Orini M, Bailón R, Mainardi LT, Laguna P, Flandrin P (2012) Characterization of dynamic interactions between cardiovascular signals by time-frequency coherence. IEEE Trans Biomed Eng 59(3):663–673
37. Karmakar C, Udhayakumar RK, Palaniswami M (2015) Distribution entropy (disten): a complexity measure to detect arrhythmia from short length rr interval time series. In: Engineering in medicine and biology society (EMBC), 2015 37th Annual International Conference of the IEEE. IEEE, pp 5207–5210

المنارة للاستشارات
www.manaraa.com

38. Tulppo MP, Makikallio T, Takala T, Seppanen T, Huikuri HV (1996) Quantitative beat-to-beat analysis of heart rate dynamics during exercise. Am J Physiol Heart Circ Physiol 271(1):H244–H252
39. Guzik P, Piskorski J, Krauze T, Schneider R, Wesseling KH, Wykretowicz A, Wysocki H (2007) Correlations between the poincaré plot and conventional heart rate variability parameters assessed during paced breathing. J Physiol Sci 57(1):63–71
40. Piskorski J, Guzik P (2005) Filtering poincaré plots. Computational Methods in Science and Technology 11(1):39–48
41. Porta A et al (2007) Assessment of cardiac autonomic modulation during graded head-up tilt by symbolic analysis of heart rate variability. Am J Physiol Heart Circ Physiol 293(1):H702–8
42. Cortes C, Vapnik V (1995) Support-vector networks. Mach Learn 20(3):273–297
43. Yan K, Zhang D (2015) Feature selection and analysis on correlated gas sensor data with recursive feature elimination. Sensors Actuators B Chem 212:353–363
44. Chang C-C, Lin C-J (2011) Libsvm: a library for support vector machines. ACM Trans Intell Syst Technol (TIST) 2(3):27
45. Silva LEV, Silva CAA, Salgado HC, Fazan R (2017) The role of sympathetic and vagal cardiac control on complexity of heart rate dynamics. Am J Physiol Heart Circ Physiol 312(3):H469–H477
46. Silva LEV, Lataro RM, Castania JA, Silva CAA, Salgado HC, Fazan Jr R, Porta A (2017) Nonlinearities of heart rate variability in animal models of impaired cardiac control: contribution of different time scales. J Appl Phys 123(2):344–351
47. Benjamini Y, Krieger AM, Yekutieli D (2006) Adaptive linear step-up procedures that control the false discovery rate. Biometrika 93(3):491–507
48. Valenza G, Nardelli M, Bertschy G, Lanata A, Scilingo E (2014) Mood states modulate complexity in heartbeat dynamics: a multiscale entropy analysis. EPL (Europhysics Letters) 107:18003
49. Cysarz D, Van Leeuwen P, Edelhäuser F, Montano N, Somers VK, Porta A (2015) Symbolic transformations of heart rate variability preserve information about cardiac autonomic control. Physiol Meas 36(4):643
50. Costa MD, Davis RB, Goldberger AL (2017) Heart rate fragmentation: a symbolic dynamical approach. Front Physiol 8:827
51. Costa M, Goldberger AL, Peng C-K (2005) Multiscale entropy analysis of biological signals. Phys Rev E 71(2):021906
52. Nardelli M, Del Piccolo L, Danzi O, Perlini C, Tedeschi F, Greco A, Scilingo E, Valenza G (2017) Characterization of doctor-patient communication using heartbeat nonlinear dynamics: a preliminary study using lagged poincaré plots. In: Engineering in medicine and biology society (EMBC), 2017 39th Annual International Conference of the IEEE. IEEE, pp 3473–3476
53. Nardelli M, Greco A, Bianchi M, Scilingo EP, Valenza G (2018) Classifying affective haptic stimuli through gender-specific heart rate variability nonlinear analysis. IEEE Transactions on Affective Computing
54. Nardelli M, Greco A, Bolea J, Valenza G, Scilingo E, Bailon R (2017) Investigation of lagged poincaré plot reliability in ultra-short synthetic and experimental heart rate variability series. In: Conference proceedings:... annual international conference of the IEEE Engineering in Medicine and Biology Society. IEEE Engineering in Medicine and Biology Society. Annual Conference, vol 2017, pp 2329–2332
55. Porta A, Gnecchi-Ruscone T, Tobaldini E, Guzzetti S, Furlan R, Montano N (2007) Progressive decrease of heart period variability entropy-based complexity during graded head-up tilt. J Appl Physiol 103(4):1143–1149
56. Silva LEV, Lataro RM, Castania JA, da Silva CAA, Valencia JF, Murta LO Jr, Salgado HC, Fazan R Jr, Porta A (2016) Multiscale entropy analysis of heart rate variability in heart failure, hypertensive, and sinoaortic-denervated rats: classical and refined approaches. Am J Physiol Regul Integr Comp Physiol 311(1): R150–R156
57. Porta A, Baselli G, Liberati D, Montano N, Cogliati C, Gnecchi-Ruscone T, Malliani A, Cerutti S (1998) Measuring regularity by means of a corrected conditional entropy in sympathetic outflow. Biol Cybern 78(1):71–78
58. Guzzetti S, Borroni E, Garbelli PE, Ceriani E, Della Bella P, Montano N, Cogliati C, Somers VK, Mallani A, Porta A (2005) Symbolic dynamics of heart rate variability: a probe to investigate cardiac autonomic modulation. Circulation 112(4):465–470
59. Brennan M, Palaniswami M, Kamen P (2001) Do existing measures of Poincaré plot geometry reflect nonlinear features of heart rate variability? IEEE Trans Biomed Eng 48(11):1342–1347
60. Spielberger CD (2010) State-trait anxiety inventory. Wiley Online Library
61. Ivanov PC, Chen Z, Hu K, Stanley HE (2004) Multiscale aspects of cardiac control. Physica A: Statistical Mechanics and its Applications 344(3-4):685–704
62. Awan I, Aziz W, Shah IH, Habib N, Alowibdi JS, Saeed S, Nadeem MSA, Shah SAA (2018) Studying the dynamics of interbeat interval time series of healthy and congestive heart failure subjects using scale based symbolic entropy analysis. PloS one 13(5):e0196823
63. Reulecke S, Villalobos SC, Voss A, González-Camarena R, González-Hermosillo JA, Gaitan J, Hernández-Pacheco G, Schroeder R, Aljama-Corrales T (2017) Temporal analysis of cardiovascular and respiratory complexity by multiscale entropy based on symbolic dynamics. IEEE Journal of Biomedical and Health Informatics

M. Nardelli received a PhD in Information Engineering from the University of Pisa (2017). Her research is mainly related to the study of nonlinear dynamics in biosignals of central and autonomic nervous systems.

A. Greco received the PhD in Automatics, Robotics and Bioengineering from the University of Pisa (2015). His main research interests are physiological modeling and biomedical signal processing.

www.manaraa.com

O. P. Danzi has achieved the Master's Degree in Applied Cognitive Psychology in 2012. From 2012, she gained experience in scientific research. From 2015, she's attending a Ph.D. course of Neuroscience, Psychology and Psychiatry at University of Verona.

E. P. Scilingo Ph.D., is Full Professor of Bioengineering at the University of Pisa. His main research interests are biomedical signal processing, wearable systems for physiological monitoring, and ICT systems for mental healthcare.

C. Perlini is a lecturer in Clinical Psychology at the University of Verona. Her main research interests include neuropsychology, rehabilitative methods, and psychophysiology.

L. Del Piccolo received her PhD in "Psychological and Psychiatric Sciences" in 1999. Her main interests are doctor-patient interaction, affective communication, and psychotherapy methods.

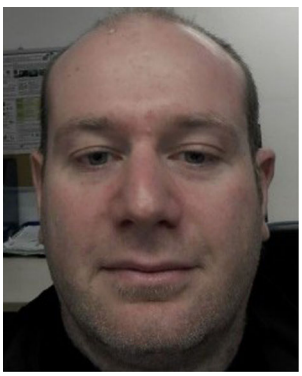

F. Tedeschi (born in 1980) received a B.Sc. (2004) and a PhD (2008) degree in Statistics in Padua; he is currently a Research Associate in the Section of Psychiatry of the University of Verona.

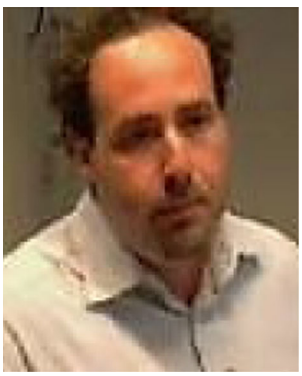

G. Valenza PhD. in Automation, Robotics, and Bioengineering, is currently an Assistant Professor of Bioengineering at the University of Pisa, with research interests in biomedical signal and image processing, cardiovascular and neural modeling, and wearable monitoring systems.

Springer
المنارة للاستشارات
www.manaraa.com

Medical & Biological Engineering & Computing is a copyright of Springer, 2019. All Rights Reserved.

www.manaraa.com